

## Two-Dimensional Coherent Double Resonance Electronic Spectroscopy

Peter C. Chen\* and Marcia Gomes

Chemistry Department, Spelman College, 350 Spelman Lane, Atlanta, Georgia 30314

Received: October 23, 2007; In Final Form: December 26, 2007

A new form of coherent 2D spectroscopy involving a pair of electronic resonances appears to provide several advantages over more established techniques. It can resolve congested peaks and sort them by vibrational quantum number, rotational quantum number, and isotopomer. The high degree of symmetry in the resulting spectra facilitates the ability to assign the quantum numbers and isotopomer for each peak. Quantitative results are demonstrated using an isotopomeric mixture of bromine.

The ability to separate and sort peaks that would otherwise appear congested in gas-phase electronic spectroscopy has recently been demonstrated using coherent 2D spectroscopy.<sup>1</sup> This capability is important because the ability to assign rotational and vibrational quantum numbers to spectroscopic peaks is often complicated by the high density of disordered and overlapping peaks produced by numerous kinds of transitions. Nonlinear techniques such as resonantly enhanced coherent anti-Stokes Raman spectroscopy (RECARS) can be used to produce two-dimensional spectra where the peaks are distributed according to rotational quantum number, rotational selection rule, and vibrational sequence.

In this paper, we explore the capabilities and potential advantages of a recently discovered form of coherent 2D spectroscopy that involves a pair of electronic resonances and that we refer to as coherent double resonance electronic (CDRE) spectroscopy. Unlike more established four wave mixing techniques such as RECARS, this new technique distributes peaks in highly symmetrical patterns.<sup>2</sup> Therefore, it may be useful for samples that are more complex and difficult to analyze, such as those containing more than one species.

The four wave mixing processes used in 2D RECARS and 2D CDRE are shown in Figure 1. Both nonlinear processes use coupling through a common rovibrational level to sort the peaks into parabolas according to rotational quantum number and selection rule. However, the common level in 2D CDRE spectroscopy is in the ground state (level a), and it organizes the parabolas into a simple square pattern (which appears rectangular in wavelength space) because both input ( $\omega_3$ ,  $y$ -axis) and output ( $\omega_4$ ,  $x$ -axis) beams probe identical sets of regularly spaced coupled vibrations in the excited state. In contrast, the RECARS process simultaneously probes vibrations in the both the ground and excited states, producing 2D spectra that contain more information, but that are more complex and less symmetrical. Furthermore, the parabolas produced in the 2D CDRE spectra are ordered by vibrational *quantum number*, whereas those in the 2D RECARS spectra are ordered by vibrational *sequence*.<sup>1</sup> This greater simplicity and higher level of symmetry

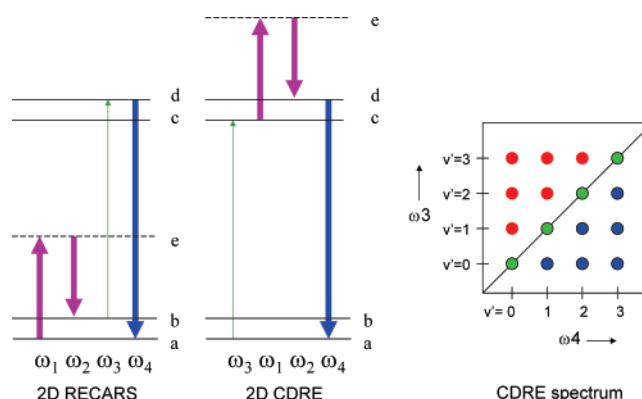


**Figure 1.** Energy level diagram for the RECARS (left) and CDRE (right) processes. Levels a and b are vibrations in the ground electronic state, and levels c and d are in the excited electronic state. Level e is a virtual level. The broad vertical arrows represent broadband input ( $\omega_1$  and  $\omega_2$ ) or broadband output ( $\omega_4$ ) fields. The box to the right shows the highly symmetrical vibrational pattern expected from a 2D CDRE spectrum.

make 2D CDRE spectroscopy more convenient for identifying and dealing with samples that are more complex.

In this paper, we use bromine to demonstrate the ability of 2D CDRE spectroscopy to spatially separate and sort peaks. Although the  $B^3\Pi_{0_v^+}$  to  $X^1\Sigma_g^+$  transition of bromine is now well-characterized,<sup>3,4</sup> its absorption spectrum has been known since around 1930 to be unusually congested and difficult to analyze due to peak overlap from three isotopomers whose natural abundance is roughly 1:2:1  $^{79}\text{Br}_2$ : $^{79,81}\text{Br}_2$ : $^{81}\text{Br}_2$ .<sup>5</sup> At room temperature, the density of absorption peaks from these isotopomers in the visible region is on the order of 1000 peaks per nm, requiring the use of very high resolution instrumentation (e.g., resolving power  $\sim 600\,000$ ) and samples comprised of pure isotopomers. An alternative approach has been to use laser induced fluorescence (LIF) spectroscopy, which provides higher selectivity than absorption spectroscopy.<sup>5</sup> However, interpreting the fluorescence spectra of the isotopomeric mixture required knowledge of accurate ground and excited-state spectroscopic constants for all three isotopomers. Furthermore, the intensity of LIF peaks can be markedly different from those predicted

\* Corresponding author. E-mail: pchen@spelman.edu. Fax: 404-270-5752.

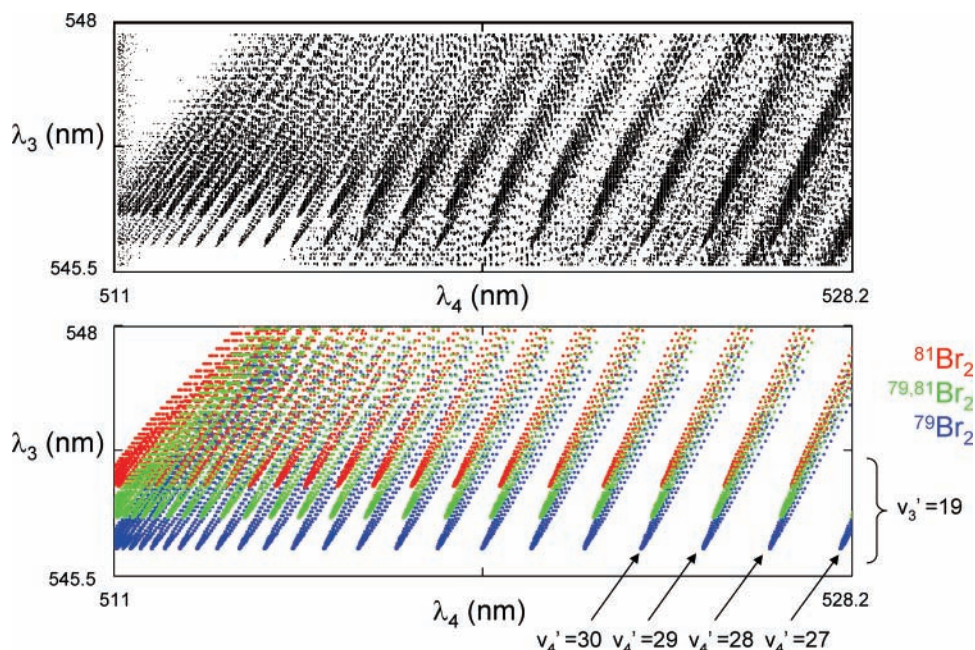


**Figure 2.** CDRE experimental (top) and simulated (bottom) contour spectra of  $\text{Br}_2$ . Note that the parabolas appear ordered by isotopomer and by vibrational quantum number:  $\nu_4'$  increases from right to left and  $\nu_3'$  increases from top to bottom. Additional peaks (not simulated) from the  $\nu_3' = 20$  parabolas can be seen rising from the bottom part of the experimental spectrum.

by absorption. In 1978 and 1980, Clyne and co-workers<sup>7,8</sup> found that the intensities of bromine's rovibrational peaks were anomalous and strongly influenced by rotationally dependent predissociation effects. Such effects make it difficult to extract quantitative and dynamical information from the intensity of LIF peaks.

Figure 2 shows a 2D CDRE contour spectrum of bromine, taken in the Anti-Stokes off-diagonal region. The experimental setup was similar to that described previously,<sup>1,2</sup> except that collinear phasematching was used instead of BOXCARS phasematching. A near-infrared beam (for  $\omega_1$  and  $\omega_2$ ) from a home-built broadband OPO was overlapped with a narrowband tunable beam ( $\omega_3$ ) from a Spectraphysics MOPO 730 ( $\sim 0.2 \text{ cm}^{-1}$  line width, running at 10 Hz). The two beams were overlapped and focused using a 200 mm FL lens. The pulse energies of the tunable narrowband and broadband beams were 1–2 and 5–10 mJ, respectively. Rejection of the input beams was achieved using Schott glass filters (KG3 and BG40) and a Kaiser holographic notch filter. The sample consisted of 0.001 atm of bromine in a 0.5 m evacuated glass cell. The resulting four wave mixing beam was focused into a 1.25 m Spex 1250m monochromator equipped with a 1200 g/mm grating, blazed at 500 nm and used in first order. The detector was a Spectrum one CCD ( $2048 \times 512$  pixels,  $13.5 \mu\text{m}$  pixel width) that provided a pixel-to-pixel resolution of 0.01 nm. The tunable OPO step size was 0.01 nm, and the integration time corresponded to 10 shots.

The 2D CDRE spectrum shows a significant improvement in resolution and peak organization compared to conventional spectra. The vast majority of the rovibrational peaks are resolved and the number of resolved peaks (approximately 10 000 in Figure 2) is more than an order of magnitude greater than the number of poorly resolved peaks observed when taking an absorption spectrum using the same 1.25 m monochromator. Spreading the peaks along a second dimension now resolves many that were previously separated by sub-Doppler (e.g., femtometers) differences (i.e., now separated along the  $\lambda_3$  axis by a distance greater than the bandwidth of the tunable OPO).

Furthermore, the peaks are now distributed into parabolas that are sequentially ordered by vibrational quantum number. Within the parabolas, the peaks are separated by rotational selection rule and sorted sequentially by rotational quantum number.<sup>1</sup>

In conventional spectroscopy, the peaks from different isotopomers crowd together and compete for space along a single one-dimensional axis. The bottom portion of Figure 2 illustrates how the different isotopomers of bromine generate distinct rows of parabolas in the coherent 2D spectrum. The location of the parabolas depends upon their vibrational spectroscopic constants, so parabolas produced by different isotopomers are shifted diagonally from one another. This shift is small compared to the vibrational constant and the distance between related isotopomer rows is small compared to the spacing between different vibrational levels. Therefore, the entire 2D spectrum (not shown here) shows periodically repeating sets of three rows (each set with a different  $\nu_3'$  value), indicating the presence of three isotopomers in the sample.

Although coherent 2D spectroscopy uses the second dimension to improve peak resolution, peak congestion remains problematic in some areas. First, the number of rotational peaks produced by the CDRE process is roughly double that of conventional spectroscopy; a  $\Delta J = \pm 1$  selection rule produces four types of peaks instead of just two: (P,P), (P,R), (R,P), and (RR). Second, the parabolas overlap severely in two regions: where  $\nu'$  is near its maximum (due to crowding of vibrational levels near the dissociation limit) and where  $\nu'$  is small (e.g., where  $\nu_4'$ , the excited-state vibration resonant with  $\omega_4$  in Figure 1, has a value  $< 27$ ). In the second region, one often observes the tail from a lighter isotopomer's parabola running into the corresponding parabola (i.e., with the same vibrational quantum numbers) from a heavier isotopomer. The clearest region appears to be near the center ( $33 < \nu_4' < 50$ ). At higher  $\nu_4'$  values ( $> 38$ ), the parabolas are also free of interference from the underlying parabolas (e.g., for Figure 2, these would be the  $\nu_3' = 20$  parabolas). Figure 3 shows a spectrum with  $\nu_4'$  in a relatively clear region. Colored simulated points calculated using constants

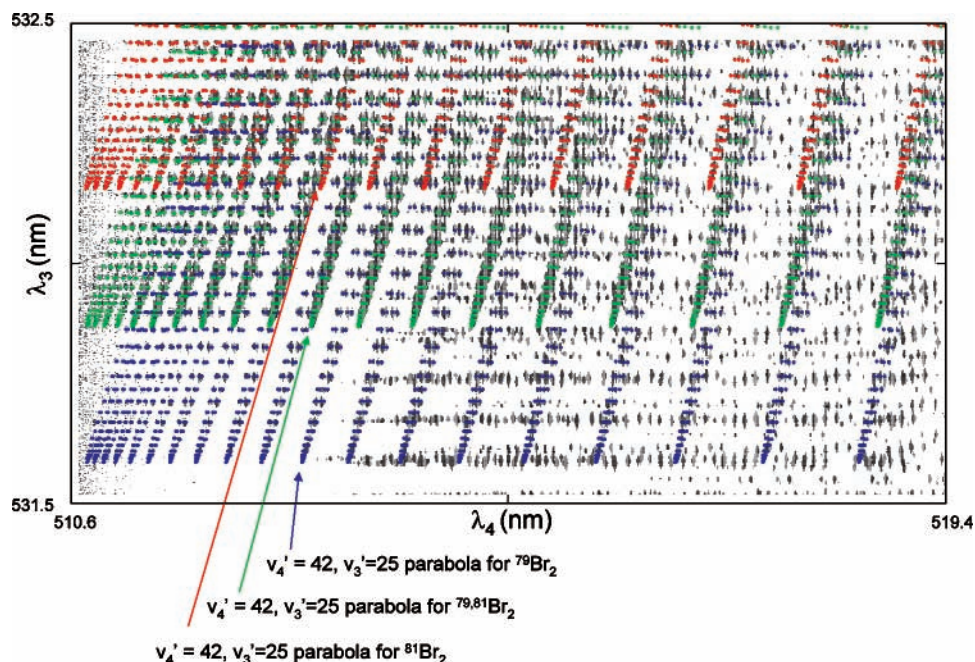


**Figure 3.** Experimental (black) peaks overlaid with simulated (colored) peaks in a relatively congestion-free region. The step size was reduced from 0.01 to 0.002 nm. Simulated peaks from underlying parabolas ( $v_3' \geq 26$ ) are not shown; their experimental counterparts appear on the middle and right (but not the left) portions of the spectrum.

from refs 3 and 4 have been laid on top of the experimental points to illustrate the level of agreement that can be achieved.

A study of the data in Figure 3 revealed quantitative and predictable peak intensity patterns. First, periodic alternations in the intensities for the peaks of  $^{79}\text{Br}_2$  and  $^{81}\text{Br}_2$ , but not for those of  $^{79,81}\text{Br}_2$ , are attributed to Fermion nuclear spin statistics (both  $^{79}\text{Br}$  and  $^{81}\text{Br}$  have nuclear spin quantum values of  $I = 3/2$ ). The experimentally observed intensity ratio of  $2.5 \pm 0.2$  (for odd:even  $J$ -valued peaks) determined from the  $v_3' = 25$ ,  $v_4' = 42$  parabola for  $^{79}\text{Br}_2$  is comparable to the value of  $(10/6)^2 = 2.78$  predicted for a coherent process. Second, the peaks from  $^{79,81}\text{Br}_2$  are more intense than those from the two other isotopomers of lower concentration. Measuring the ratio of the  $^{79}\text{Br}_2$  or  $^{81}\text{Br}_2$  peak intensity over that of the  $^{79,81}\text{Br}_2$  peak is somewhat complicated by odd/even rotational alternations in the height of the  $^{79}\text{Br}_2$  and  $^{81}\text{Br}_2$  peaks attributed to nuclear spin statistics. The measurements (again using peaks from the  $v_3' = 25$ ,  $v_4' = 42$  parabola,  $J''$  from 11 to 24) yielded average peak heights of  $5.1 \pm 1.1$  for the  $^{79,81}\text{Br}_2$  peaks and  $1.29 \pm 0.65$  for the  $^{81}\text{Br}_2$  peaks (in arbitrary units). The peak intensities were corrected for thermal population and degeneracy effects, and the larger relative standard deviation for the  $^{81}\text{Br}_2$  peaks is attributed to the alternation effect. The ratio of the two resulting peak intensity averages ( $5.1/1.29 = 3.9$ ) is in good agreement with the predicted value of 3.8 based on the square of the isotopomer population ratio.

A third observed intensity trend is that the PP and RR peaks are both twice the intensity of the mixed PR and RP peaks. One factor that could influence the relative size of these peaks is the number of virtual levels; the mixed peaks can only involve virtual states that have the same rotational quantum number as the initial state, whereas the virtual states of the PP and RR peaks can have rotational quantum numbers that differ from that of the initial state by 0 or 2 quanta. However, simply doubling the number of virtual states should increase the observed intensity by a factor of 4. These results suggest a need

for further studies that take into consideration additional effects such as interference.

In conclusion, 2D CDRE spectroscopy improves spectral resolution and sorts peaks by rotational and vibrational quantum number. The highly symmetric patterns in the resulting spectra help facilitate the detection of multiple isotopomers and the separation and sorting of their peaks. In contrast, the existence of isotopomers seriously complicates conventional spectra because of the large amount of information that is crowded onto a single axis. The intensities of peaks in the 2D CDRE spectra fit predictions made according to nuclear spin statistics and population ratios. These results suggest that this technique should be a strong candidate for future studies on the dynamics and kinetics of molecular systems, where the complexity of the spectra can increase to the point where the analysis becomes prohibitively difficult when using conventional forms of spectroscopy.

**Acknowledgment.** This work was supported by National Science Foundation Grant CHE-0616661. Additional support was provided by NIH Grant MD-02-005 and NSF grant EEC-0310717. We express our gratitude to Professor Michael Heaven for his helpful comments regarding bromine fluorescence.

## References and Notes

- (1) Chen, P. C.; Joyner, C. C. *Anal. Chem.* **2005**, *77*, 5467–5473.
- (2) Chen, P. C.; Joyner, C. C. *J. Phys. Chem.* **2006**, *110*, 7989–7993.
- (3) Gerstenkorn, S.; Luc, P.; Raynal, A.; Sinzelle, J. *J. Phys. (Paris)* **1987**, *48*, 1685–1696.
- (4) Gerstenkorn, S.; Luc, P. *J. Phys. (Paris)* **1989**, *50*, 1417–1432.
- (5) Focsa, C.; Li, H.; Bernath, P. F. *J. Mol. Spectrosc.* **2000**, *200*, 104–119.
- (6) Barrow, R. F.; Clark, T. C.; Coxon, J. A.; Yee, K. K. *J. Mol. Spectrosc.* **1974**, *51*, 428–449.
- (7) Clyne, M. A. A.; Heaven, M. C. *J. Chem. Soc., Faraday Trans. 2*, **1978**, *74*, 1192–2013.
- (8) Clyne, M. A. A.; Heaven, M. C.; Martinez, E. *J. Chem. Soc., Faraday Trans. 2*, **1980**, *76*, 405–419.